HardwareX 14 (2023) e00416

Contents lists available at ScienceDirect

HardwareX

journal homepage: www.elsevier.com/locate/ohx

Quartz crystal Microbalance with dissipation monitoring for biomedical applications: Open source and low cost prototype with active temperature control

G.G. Muñoz [a], M.J. Millicovsky [a,b], J.M. Reta [a], J.I. Cerrudo [a], A. Peñalva [a], M. Machtey [a], R.M Torres [c], M.A. Zalazar [a,b,*]

[a] Facultad de Ingeniería, Universidad Nacional de Entre Ríos, Ruta Prov. 11 (Km 10), (3100) Oro Verde, Entre Ríos, Argentina
[b] Instituto de Investigación y Desarrollo en Bioingeniería y Bioinformática – Consejo Nacional de Investigaciones Científicas y Técnicas, Facultad de Ingeniería, Universidad Nacional de Entre Ríos, Ruta Prov. 11 (Km 10), (3100) Oro Verde, Entre Ríos, Argentina
[c] R.O.M.A.T. Creator Center. Colonia Avellaneda. Entre Ríos, Argentina. Investigador independiente, colaborador de la Facultad de Ingeniería, Universidad Nacional de Entre Ríos, Ruta Prov. 11 (Km 10), (3100) Oro Verde, Entre Ríos, Argentina

ARTICLE INFO

Article history:
Received 26 December 2022
Received in revised form 14 March 2023
Accepted 29 March 2023

Keyword:
Biomedical applications
Quartz Crystal Microbalance
Dissipation monitoring
Temperature control

ABSTRACT

Advances in sensors have revolutionized the biomedical engineering field, having an extreme affinity for specific analytes also providing an effective, real-time, point-of-care testing for an accurate diagnosis. Quartz Crystal Microbalance (QCM) is a well-established sensor that has been successfully applied in a broad range of applications to monitor and explore various surface interactions, in situ thin-film formations, and layer properties. This technology has gained interest in biomedical applications since novel QCM systems are able to work in liquid media. QCM with dissipation monitoring (QCM-D) is an expanded version of a QCM that measures changes in damping properties of adsorbed layers thus providing information on its viscoelastic nature. In this article, an open source and low cost QCM-D prototype for biomedical applications was developed. In addition, the system was validated using different Polyethylene Glycol (PEG) concentrations due to its importance for many medical applications. The statistics show a bigger dissipation of the system as the fluid becomes more viscous, also having a very acceptable sensibility when temperature is controlled.

Specifications table

Hardware name	QCM prototype
Subject area	• Engineering and material science • Sample handling and preparation • Open source alternatives

(*continued on next page*)

* Corresponding author at: Facultad de Ingeniería, Universidad Nacional de Entre Ríos, Ruta Prov. 11 (Km 10), (3100) Oro Verde, Entre Ríos, Argentina.
E-mail address: martin.zalazar@uner.edu.ar (M.A. Zalazar).

https://doi.org/10.1016/j.ohx.2023.e00416
2468-0672/

(*continued*)

Hardware name	QCM prototype
Hardware type	• Measuring physical properties and point-of-care sensors • Field measurements and sensors • Electrical engineering and computer science
Closest commercial analog	• openQCM NEXT • QSense Pro (Biolin Scientific)
Open source licence	*Creative Commons Attribution 4.0 International*
Cost of hardware	*$ 605.5*
Source file repository	https://doi.org/10.5281/zenodo.7733393

Hardware in context

The use of sensors in the world is on the rise, providing information on medical diagnostics for health care and improving quality of life [1]. Acoustic sensor systems, such as the quartz crystal microbalance (QCM) have shown versatility in chemical, physical, biological and biomedical research [2]. The QCM technique has traditionally been used to monitor mass or thickness of thin films deposited on surfaces and to study gas [3]. This device gained interest in the biomedical field since 1980s when novel QCM systems started to work in liquid media being implemented on several applications [4–7]. The crystal is fabricated using growing gold or platinum films (electrodes) on the surface of a thin AT-cut quartz crystal disc [8]. The characteristics of this sensor are highly dependent on the chemical nature and physical properties of the sensing material that covers the active electrode [9].

The QCM operation consists of performing a frequency sweep, generally with a vector network analyzer (VNWA) [10], to make the crystal oscillate at its fundamental resonance frequencies and its overtones. The instrument obtains the scattering (S) parameters from the reflected signal (S11 parameter) [11]. Mass depositing onto the sensor surface is detected in real time as negative frequency shifts on QCM natural resonance frequency [12]. The extended QCM-D version allows measurements of dissipative energy (D) arising from the dampening of the crystal's oscillation by the adsorbed layer of material, thus providing information on its viscoelastic nature [13]. Dissipation is the inverse of the quartz crystal quality factor (Q), being the ratio of resonant frequency and full width at half maximum (FWHM) [14]; it also can be observed on the real part of admittance parameter Y11 from S11 parameter [15,16].

When the crystal is in contact with liquids, both the accumulation of rigid mass and changes in the liquid properties, e.g., density and viscosity, contribute to the frequency shift [17] and have a strong dependence on temperature. Controlling temperature effects is significant when high accuracy measurements are desired [17,18]. In addition, oscillation frequency stability of the quartz crystal is affected by changes in temperature, impacting on the robustness and reproducibility of the measurements causing resonance frequency shifts [18–20]. Temperature is controlled with an active Peltier-based temperature system [21] in a closed chamber to achieve temperature stability [22]. A proportional, integral and derivative (PID) controller is used allowing a good control of time response, response accuracy, and helping to improve the prior and inherent errors of the system, also adding an automatic tuning and prediction system [23].

Typical QCM-D designs have a sensor case that provides crystal security while measuring and inserting the samples [24]. The case also supplies a connection to the measuring instrument and silicone O-rings seal to avoid electrical shortcuts [25]. The mounting and placement of the crystal is critical and the operation and sensitivity of the QCM are highly dependent on them [26]. Custom QCM systems still remain popular to suit specific experiments, and commercial systems aim to maximize electrical and thermal performances with high quality components, expensive, and bulky lab-based high frequency analyzers [27]. Researchers from Novaetech S.R.L. created the Open QCM project, which consists of developing the necessary tools to carry out research work with QCM. Based on this, an inexpensive and open source QCM-D prototype designed for biomedical applications was developed. The prototype quality for biomedical applications was validated by analyzing the viscosity of different electrolyte solutions of PEG 3350 (Elea), which is a condensation polymer of ethylene oxide and water, being used for vast applications, as medical, chemical and biological.

Hardware description

A lightweight and compact QCM-D system was developed (Fig. 1). A printed circuit board (PCB) with pogo-pins associates the quartz crystal electrodes to a VNWA. In addition, an active proportional–integral–derivative (PID) temperature control system, implemented with a Raspberry Pi board, controls a Peltier cell.

Sensor case

The sensor case was designed on Autodesk Fusion 360 and printed with a 3D printer (Creality LD-006) by using UV sensitive resin, having a width of 44 mm, a length of 40 mm, a height of 15 mm, and a weight of 21.5 gr (Fig. 2). KiCad open-source software suite for electronic engineering was used to design a one-layer PCB, allowing the VNWA (Model

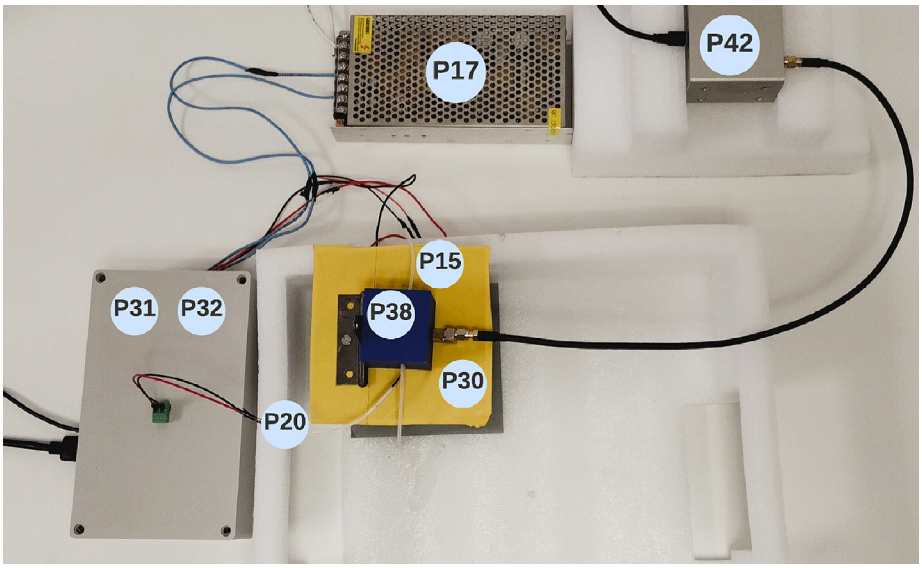

Fig. 1. Overview of the QCM-D System. Parts are detailed in Section 4 (Bill of materials).

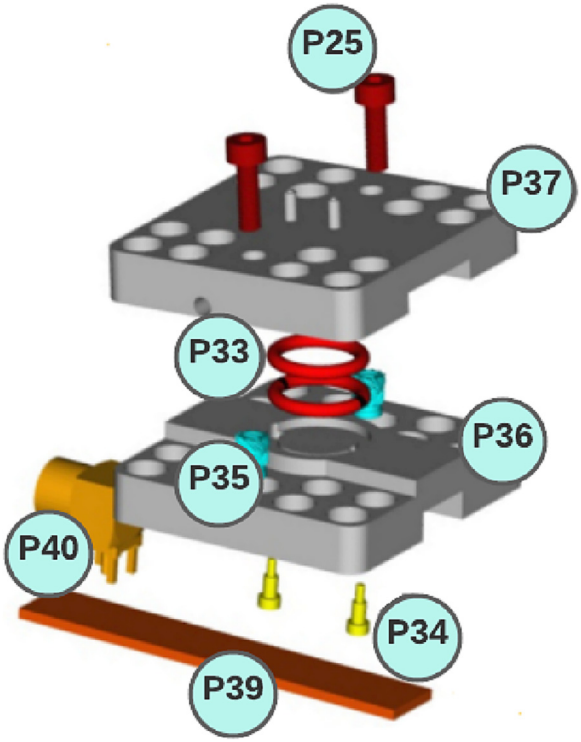

Fig. 2. Exploded view of the sensor case. The parts are detailed in Section 4 (Bill of materials).

DG8SAQ, SDR-Kits) to perform measurements on the crystal (Fig. 3). Electrical connection was done through SMA connectors (Amphenol, low noise) and gold-planted pogo-pins. The upper part of the case provides a hermetic closure while connected to the hoses through two rigid nipples. Sensor case was set for undemanding maintenance providing both, quick and easy crystal positioning. The crystal is in contact with a silicone O-ring that stabilizes the pressure on the crystal and also prevents liquid from spilling out. A ventilation system for optimizing temperature distribution inside the case was added.

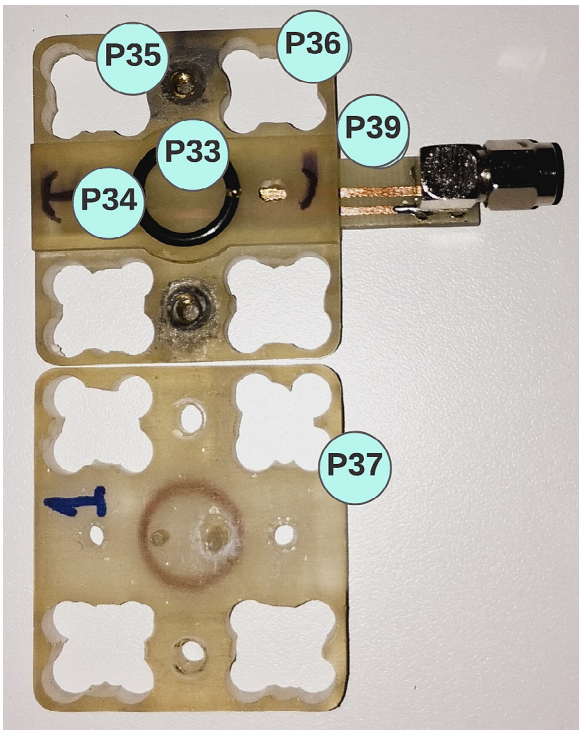

Fig. 3. 3D printed sensor case. Parts are detailed in Section 4 (Bill of materials).

Temperature control system

Peltier cell

A Peltier cell (TEC1-12706) supplied with 12V and 6A, was selected as the thermoelectric device. An aluminum heat sink, together with thermal grease and a fan, favor the temperature difference between both Peltier faces. Thermal control has a 18 °C−30 °C nominal working range, and bidirectional heating and cooling. 3D printed polylactic acid (PLA) accessories were made to protect the fan, divide the Peltier from the sensor case, and cover the whole sensor case working as a thermal insulator as shown in Fig. 4.

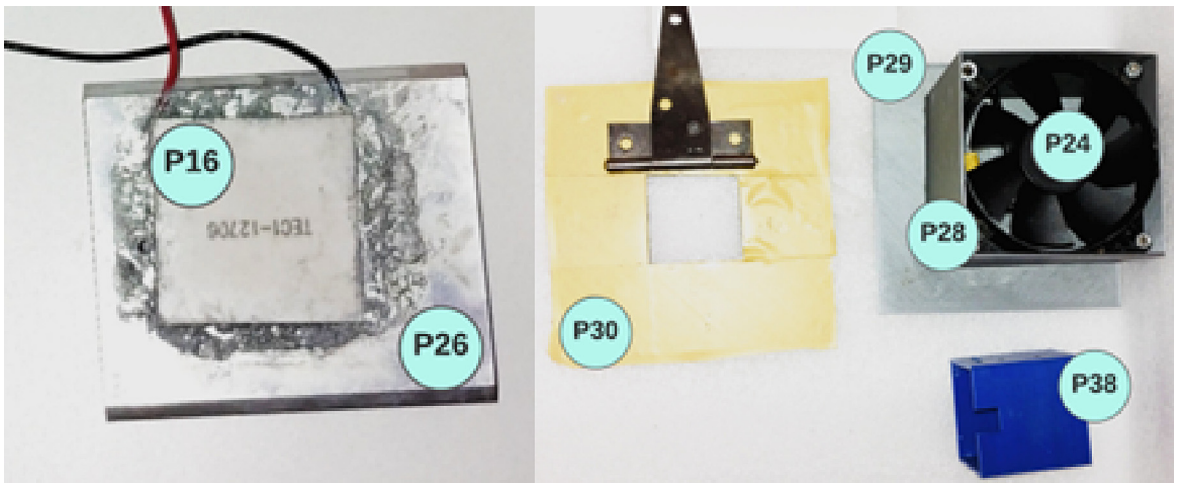

Fig. 4. Peltier Cell with heat sink and Fan with plastic accessories. Parts are detailed in Section 4 (Bill of materials).

PID temperature control

Raspberry Pi 4 Model B was selected as the microcontroller for PID control since it is free to use (Fig. 5). Temperature acquisition starts with a thermistor (NTC 3950) providing fast response time and precision. Because of the absence of Analog to Digital Converters (ADCs) on the Raspberry, the voltage difference acquired by the NTC needs to be converted as digital data at the microcontroller by an ADC (MCP3008). PID program was implemented with Python, being an open source and commonly used language that suits the temperature control code. The Peltier cell current was driven through a Pulse Width Modulation (PWM) Raspberry signal by using a "H" bridge 2-channel stepper motor driver (VNH2SP30 30 Amp). A switching power supply (12V-10A) was chosen to supply the driver, fan, and Peltier cell, while the Raspberry was supplied through an USB PC port.

Acquisition system

The used piezoelectric crystal was a 10 MHz AT-cut suitable for liquid biosensing (Novaetech Srl), having a flat crystal surface carefully polished. It has a thickness of 160 um and a nominal sensitivity of 4.42 × 10–9 g Hz-1 cm-2. For the gold electrodes, a titanium adhesion layer was used, Diameters of the front and back electrodes (single side) are 11.5mm and 6mm respectively.

A vector network analyzer (DG8SAQ 3, SDR-Kits) (Fig. 6) was selected for measurement of S11 parameter (Fig. 7) and can be transformed to an impedance (Z) or admittance (Y) parameter on the VNWA software to obtain the desired conductance. The software application provided by the manufacturer allows a frequency sweep of 1 kHz−.3 GHz and can measure up to 65,000 data points with a sampling time ranging from 0.13 ms−100ms. Data can be exported as a Touchstone format archive.

Design files summary

Design Filename	File type	Open source license	Location of the file
P1 - Bottom_part_S_case.stl	3D Printing	Creative Commons Attribution 4.0 International	https://doi.org/10.5281/zenodo.7733393
P2 - Top_part_S_case.stl	3D Printing	Creative Commons Attribution 4.0 International	https://doi.org/10.5281/zenodo.7733393
P3 - Cover_S.stl	3D Printing	Creative Commons Attribution 4.0 International	https://doi.org/10.5281/zenodo.7733393
P4 - Cover_Fan.stl	3D Printing	Creative Commons Attribution 4.0 International	https://doi.org/10.5281/zenodo.7733393
P5 - P_S_Divisor.stl	3D Printing	Creative Commons Attribution 4.0 International	https://doi.org/10.5281/zenodo.7733393
P6 - Base_Fan.stl	3D Printing	Creative Commons Attribution 4.0 International	https://doi.org/10.5281/zenodo.7733393
P7- Top_cabinet_T	3D Printing	Creative Commons Attribution 4.0 International	https://doi.org/10.5281/zenodo.7733393
P8- Base_cabinet_T	3D Printing	Creative Commons Attribution 4.0 International	https://doi.org/10.5281/zenodo.7733393
P9 - QCM_SMA.kicad_pcb	PCB design	Creative Commons Attribution 4.0 International	https://doi.org/10.5281/zenodo.7733393
P10- Temperature_Control_Sensor.py	Software	Creative Commons Attribution 4.0 International	https://doi.org/10.5281/zenodo.7733393
P11-Temperature_Control_PWM.py	Software	Creative Commons Attribution 4.0 International	https://doi.org/10.5281/zenodo.7733393
P12-Temperature_Control_Interface.py	Software	Creative Commons Attribution 4.0 International	https://doi.org/10.5281/zenodo.7733393
P13-Temperature_Control_Main.py	Software	Creative Commons Attribution 4.0 International	https://doi.org/10.5281/zenodo.7733393
P14-Temperature_Control_PID.py	Software	Creative Commons Attribution 4.0 International	https://doi.org/10.5281/zenodo.7733393

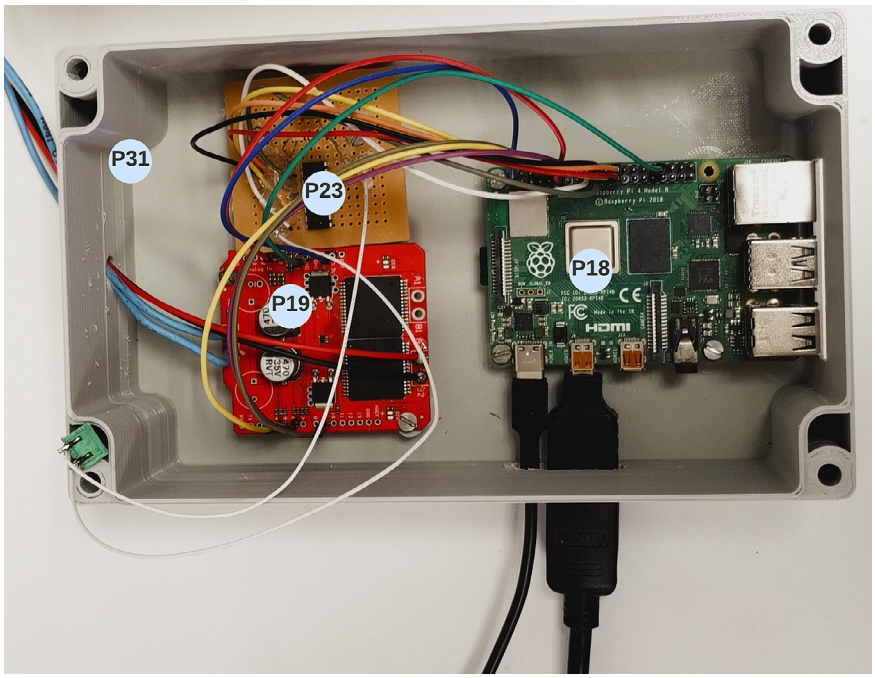

Fig. 5. PID Temperature Control devices. Parts are detailed in Section 4 (Bill of materials).

Fig. 6. VNWA for measurement of S parameters.

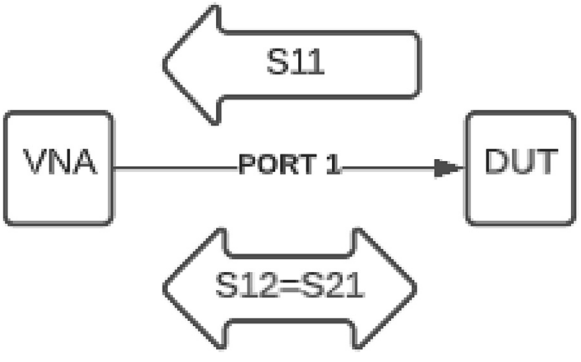

Fig. 7. One port network graph for S parameters.

Bill of materials summary

Designator	Component	Number	Cost per Unit- USD	Total cost-USD	Source of materials	Material type
P15	Hose	1	$6.00	$6.00	AMAZON	Silicone
P16	Peltier Cell TEC1-12706	1	$9.00	$9.00	DIGIKEY	Semiconductor
P17	Power supply 12V/10A	1	$19.96	$19.96	AMAZON	Other
P18	Raspberry Pi 4 Model B	1	$75.00	$75.00	DIGIKEY	Other
P19	VNH2SP30 30A 2-channel stepper motor driver	1	$21.71	$21.71	UNIBOT	Other
P20	NTC 3950 analog sensor	1	$0.64	$0.64	DIGIKEY	Semiconductor
P21	Resistor 100 KOhm	1	$0.03	$0.03	DIGIKEY	Other
P22	Ceramic capacitor 220 nF	1	$0.03	$0.03	AMAZON	Ceramic
P23	MCP3008 A/D converter	1	$3.21	$3.21	MOUSER	Other
P24	Fan	1	$13.24	$13.24	DIGIKEY	Other
P25	Screw	2	$0.12	$0.24	DIGIKEY	Metal
P26	Heat sink	1	$10.65	$10.65	DIGIKEY	Metal
P27	Thermal grease	1	$20,31	$20,31	MOUSER	Polymer
P28	*Cover_Fan_PLA	1	$24.69	$24.69	AMAZON	Polymer
P29	*Base_Fanl_PLA	1	$24.69	$24.69	AMAZON	Polymer
P30	*Divisor_PLA	1	$24.69	$24.69	AMAZON	Polymer
P31	*Base_cabinet	1	$24.69	$24.69	AMAZON	Polymer
P32	*Top_cabinet	1	$24.69	$24.69	AMAZON	Polymer
P33	O-Ring	2	$0.36	$0.72	EBAY	Polymer
P34	Pogo-Pin	2	$0.80	$1.60	DIGIKEY	Metal
P35	Inserts	2	$0.08	$0.17	AMAZON	Metal
P36	^Bottom_part_Resin	1	$37,58	$37,58	AMAZON	Polymer
P37	^Top_part_Resin	1	$37,58	$37,58	AMAZON	Polymer
P38	*Cover_S_PLA	1	$24.69	$24.69	AMAZON	Polymer
P39	PCB	1	$13.99	$13.99	AMAZON	Other
P40	SMA connector	1	$10.66	$10.66	MOUSER	Metal
P41	Glue	1	$3.13	$3.13	DIGIKEY	Other
P42	Vector Network Analyzer v3 DG8SAQ	1	$305.88	$305.88	SDR-Kits	Semiconductor
P43	Crystal open QCM 10 MHz	10	$26.85	$268,55	openQCM	Other

*3D printed parts with PLA, a single 1.75mm 1kg PLA filament was used, its cost is $24.69.
^3D printed parts with resin.

The full version of the Bill of Materials that contains electronic components detail is available with the supplementary material (https://doi.org/10.5281/zenodo.7733393).

Build instructions

Materials and tools

Refer to the bill of materials (Section 4) for a sorted list of materials. STL files provided are intended to be 3D printed. Building the device requires access to some basic tools:
-Soldering iron
-Tin lead solder wire
-Wire cutters
-Screwdrivers
-Tweezers
-Multimeter

Sensor case construction

Step 1: Make the printed circuit boards (P9). This can be done on your own or sending the designs to a PCB manufacturing company.

Step 2: Solder the SMA connector (P40) and pogo-pins (P34) on the PCB.
Step 3: Print the pieces (P1, P2) with a 3D printer.
Step 4: Attach the soldered PCB (made in step 2) to the sensor case base (P36) using glue (P41).
Step 5: Insert O-Rings (P33) into the base and the upper part of the sensor. Press the O-Rings.
Step 6: Insert two pogo pins (P34) where the lower O-ring sits.
Step 7: Place two inserts (P35) in P36.
Step 8: Perform a leak test. Before liquid adding, insert two strips of paper between case parts and wait one hour to identify if papers are wet (Fig. 8).

Temperature control

Step 1- Solder MCP3008 A/D converter (P23) on a PCB and connect these components:

- 200 pF ceramic Capacitor (P22) between CH7-GND of MCP3008
- 100K Ohm Resistor (P21) between CH7-GND of MCP3008
- NTC 3950 analog sensor (P20) between CH7-VDD of MCP3008

Step 2: Connect MCP3008 (P23) to Raspberry Pi (P18) via SPI and follow these connections:

- MCP3008 VDD to Raspberry Pi 3.3V (pin 17)
- MCP3008 VREF to Raspberry Pi 3.3V (pin 17)
- MCP3008 AGND to Raspberry Pi GND (pin 20)
- MCP3008 DGND to Raspberry Pi GND (pin 20)
- MCP3008 CLK to Raspberry Pi (pin 23)
- MCP3008 DOUT to Raspberry Pi (pin 21)
- MCP3008 DIN to Raspberry Pi (pin 19)
- MCP3008 CS/SHDN to Raspberry Pi (pin 24)

Step 3: Connect VNH2SP30 motor driver (P19) to the Raspberry Pi (P18) making the following connections:

- VNH2SP30 GND to Raspberry Pi GND (pin 34)
- VNH2SP30 +3.3 V to Raspberry Pi 3.3V (pin 1)
- VNH2SP30 EN1 to Raspberry Pi (pin 10)
- VNH2SP30 B2 to Raspberry Pi (pin 5)
- VNH2SP30 A2 to Raspberry Pi (pin 8)
- VNH2SP30 PWM2 to Raspberry Pi (pin 9)

Step 4: Connect VNH2SP30 motor driver (P19) to power supply (P17).
Step 5: Connect Peltier cell (P16) to VNH2SP30 motor driver (P19) A1:B1.
Step 6: Screw the fan (P24) with four support screws (P25).
Step 7: Mount the heat sink (P26) above the fan (P24).
Step 8: Apply thermal grease (P27) between the Peltier cell (P16) and the heat sink (P26). Then mount the Peltier cell (P16) above the heat sink (P26).
Step 9: 3D-Print the fan and sensor case plastic support parts (P3, P4, P5, P6). On the other hand, 3D-print the cabinet (P7, P8).
Step 10: Insert the temperature sensor (P20) into the cover (P38) and then into the sensor case (P36, P37).

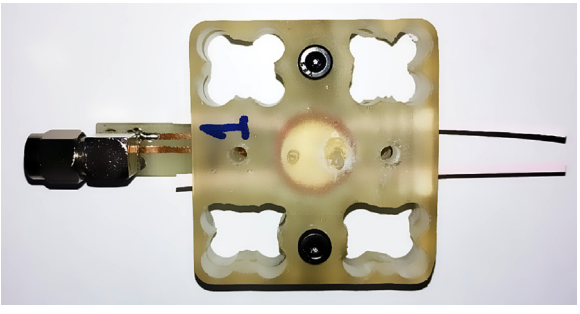

Fig. 8. Two paper strips located inside the sensor case were used for the leak test.

Step 11: Set up the Raspbian operating system using the document described by the Raspberry Pi Foundation (https://projects.raspberrypi.org/en/projects/raspberry-pi-getting-started).

Step 12: Connect the Raspberry board (P18) to the PC via USB port and open IDE.

Step 13: Load script "Temperature_Control_Interface.py" (P12). The file has to be in the same folder as the other files with extension.py (P10, P11, P13, P14).

Step 14: On Interface, select temperature. Then select time.

Step 15: Compile and Upload the firmware to the microcontroller.

Operation instructions

Before doing any experiment, a calibration for one port operation must be done on VNWA. The process uses different loads: short, open and 50 O SMA accessories (Fig. 9).

Once the measuring instrument is calibrated, the crystal must be cleaned according to the required protocol. Then, the crystal is placed on the O-ring of the upper case by using plastic tweezers, thus preventing excessive pressure and a crystal break. The case is closed with screws ensuring a constant pressure. The cannula connected to a syringe reaches the sensor case by means of a hose in the cover (Fig. 10). Finally, the cover is located and the VNWA is connected to start the acquisition.

Temperature control system software is accessed using peripherals. These are connected to the Raspberry having a simple and friendly user interface for easy handling. Time and temperature can be set once the program is loaded by typing the value in the text box and pressing the set button (Fig. 11). Once the temperature and time have been set, the controller starts to work by pressing the main button. While temperature is controlled, the main button remains on its original state until time reaches zero.

The VNWA software (Fig. 12) allows to observe graphs in real time and exports the frequency sweep data in Touchstone format for later analysis by the free program R-studio.

Fig. 9. VNWA calibration tools.

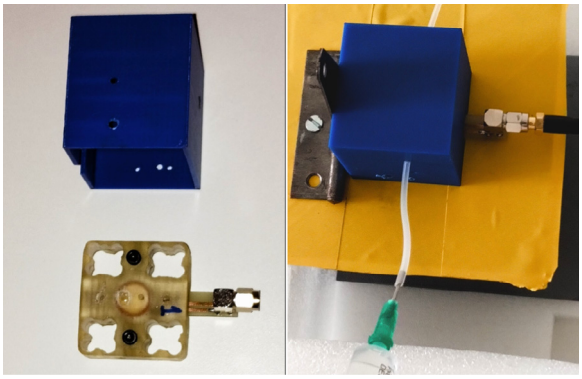

(a) (b)

Fig. 10. (a) Hoses, sensor case and cover. (b) Sensor case assembly and syringe connection.

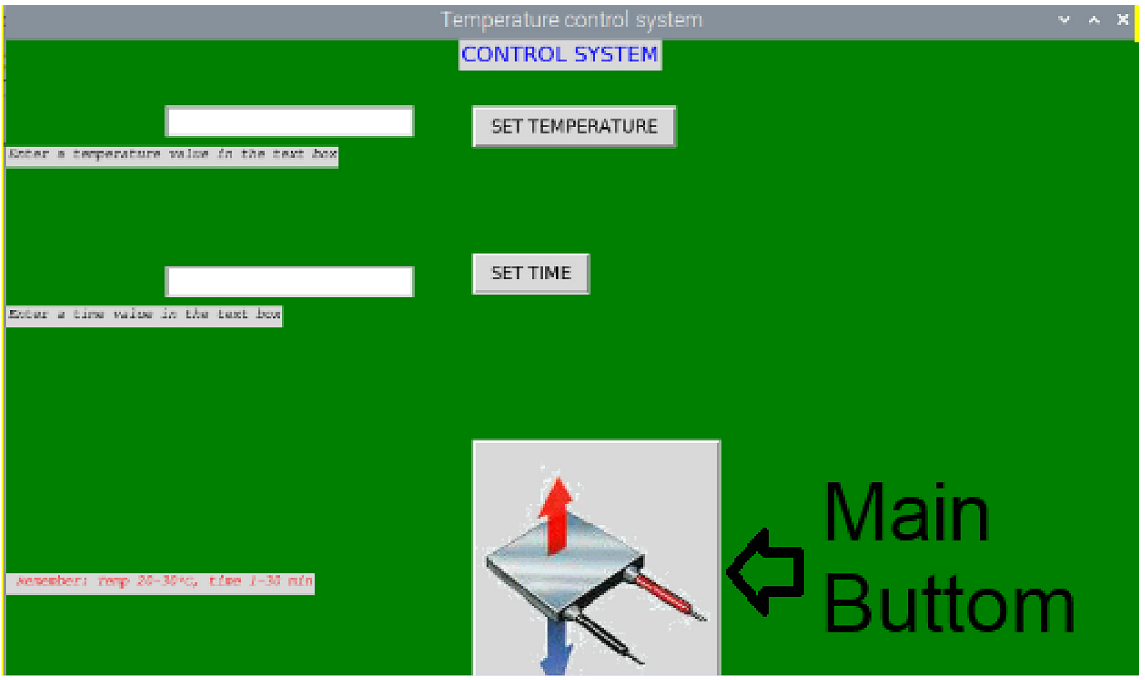

Fig. 11. Temperature control system graphical user interface.

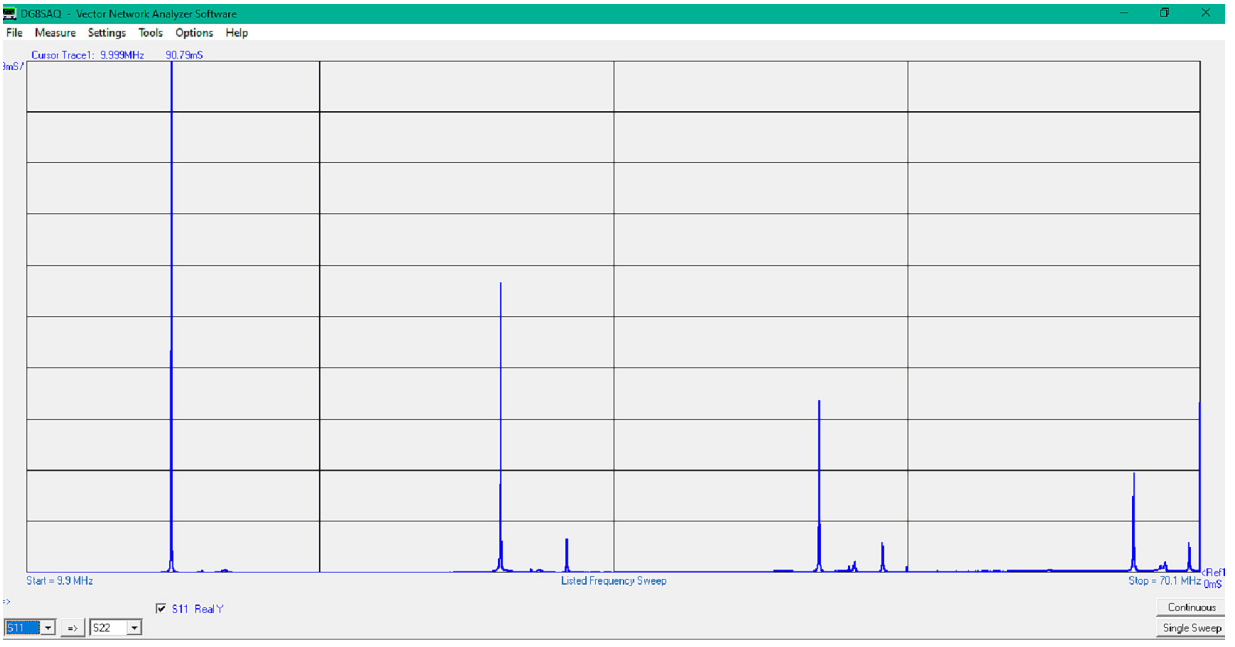

Fig. 12. VNWA DG8SAQ3 software graphical user interface.

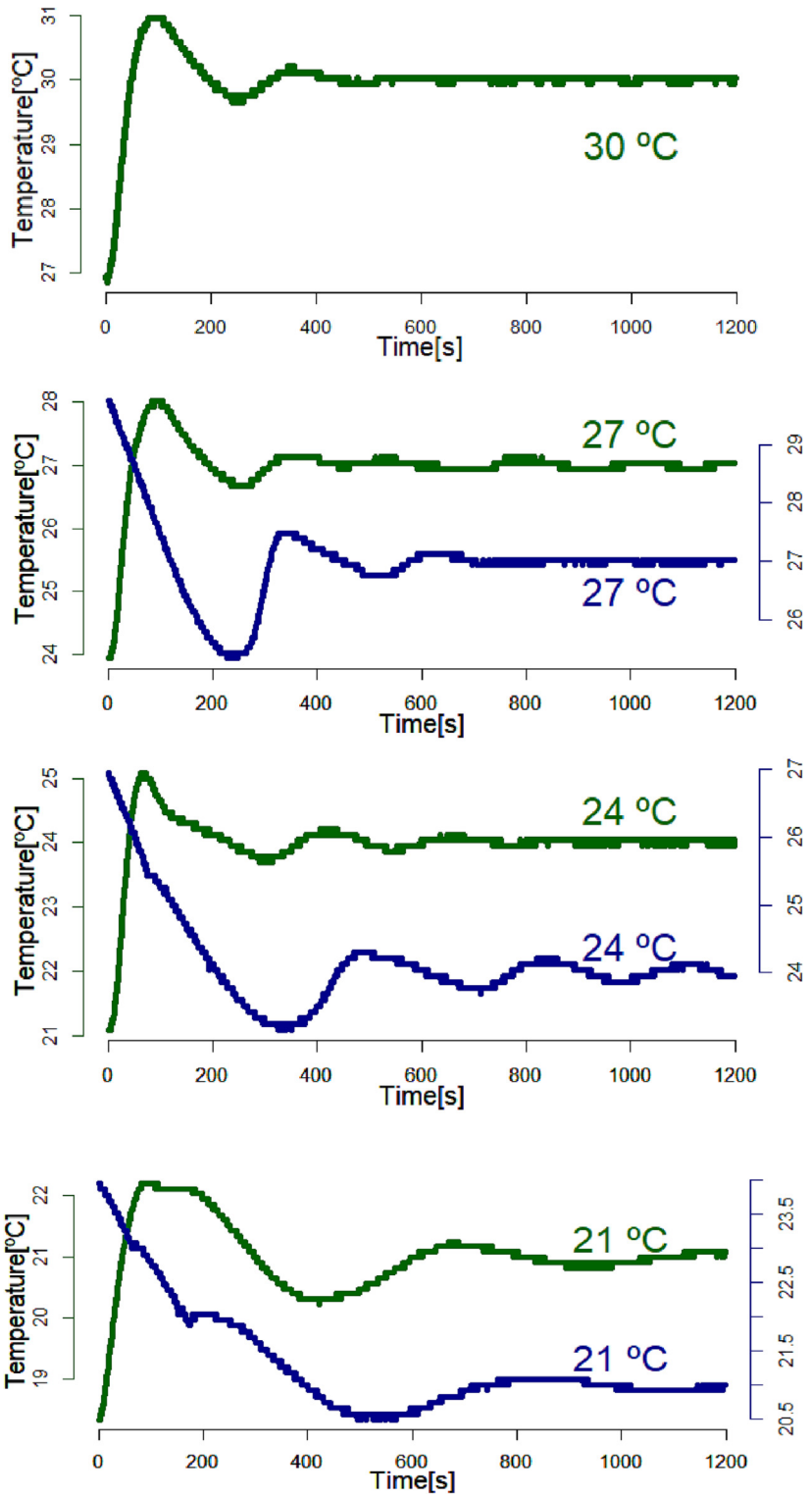

Fig. 13. Response of the temperature control system. Green: from a lower temperature to a desired value. Blue: from a higher temperature to a desired value. (For interpretation of the references to colour in this figure legend, the reader is referred to the web version of this article.)

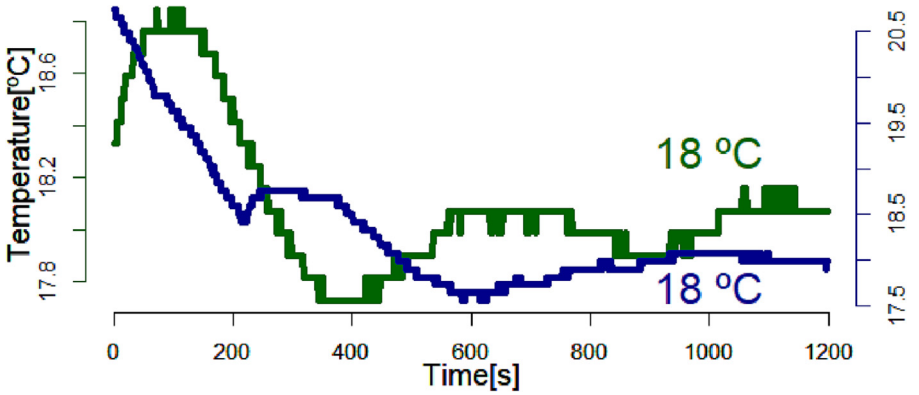

Fig. 13 (*continued*)

Results

Characterization

Temperature stability

NTC was placed as close as possible to the crystal and the test consists of sweeping the temperature from 18 °C to 30 °C and vice versa by 3 °C (Fig. 13) steps in a 20 min process.

The device presents a temperature stability time of 10 min with a long-term stability of 0.1< °C/h.

Crystal cleaning

Crystal was cleaned (Fig. 14) with 2% SDS detergent for 5 min, rinsed with distilled water and dried with pure nitrogen gas (Fig. 15).

Experimental design

Ten measurements, both in air and water at five temperatures (18°C, 22°C, 26°C, 30°C, no control (NC)) were taken (Fig. 16, Fig. 17). The experiment was replicated three times giving a total of 300 measurements (Fig. 18).

The results were expected to be stable over the entire temperature range, and the most stable temperature was 26°C. This temperature was defined as the working temperature and the fundamental resonance frequency obtained was 9.998957 MHz. Furthermore, long-term stability values were obtained for the fundamental frequency (1.1 Hz/h) and the dissipation (1.7 E-12/h).

Validation

Validation was performed by measuring the resonance frequency and dissipation of different concentrations of PEG 3350 (5%, 10% and 20%). Crystal cleaning was done before taking measurements. Every time the sample was changed, the crystal was rinsed with distilled water, injecting a volume of approximately 1.5 ml to eliminate any remaining PEG on surface.

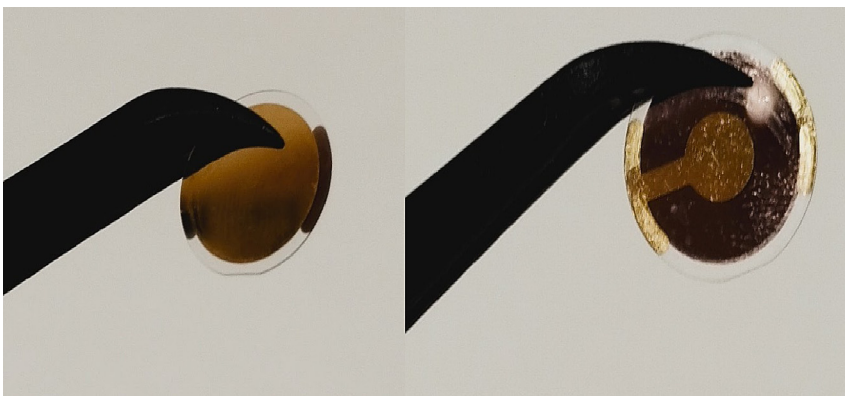

Fig. 14. Crystal front and back electrodes.

Fig. 15. Crystal cleaning elements.

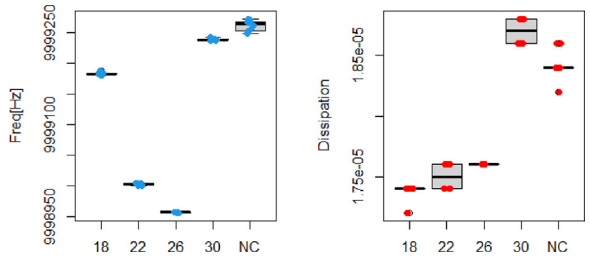

Fig. 16. Study of variability of frequency and dissipation in air with different control temperatures.

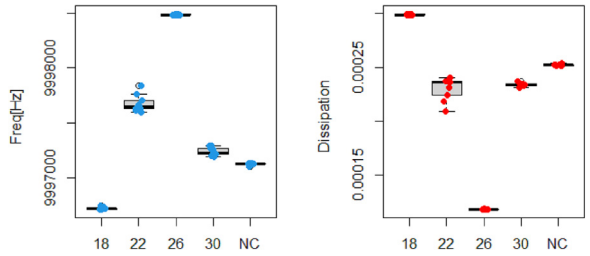

Fig. 17. Study of variability of frequency and dissipation in water with different control temperatures.

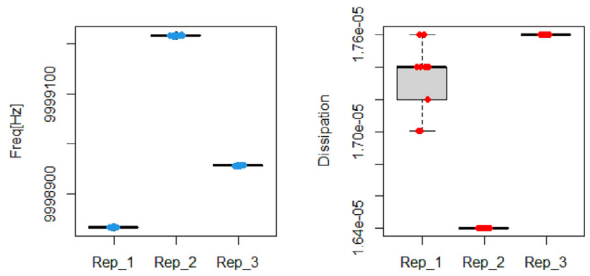

Fig. 18. Resonance Frequency and Dissipation replicate comparison at 26 °C.

PEG solutions show significant difference with respect to dissipation ($p< 6.02e-06$) and frequency ($p< 0.000176$), and an increase in dissipation and frequency variation can be seen as the PEG concentration increases (Fig. 19). Results present a greater variability than expected regarding the marked difference between PEG concentrations.

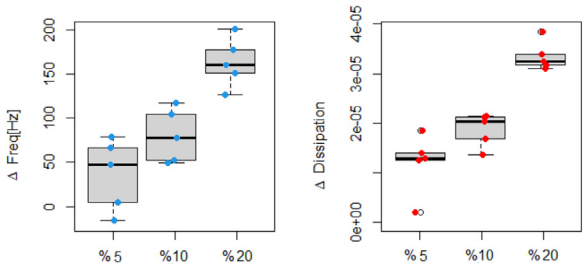

Fig. 19. Variation of F0 and D0 as a function of the change in PEG concentration.

Discussion and conclusion

In this article, an open source and low cost QCM-D prototype for biomedical applications with active temperature control was presented. It was made up of simple and high-quality parts that allow the user to set up the device and its handling in an easy way. The characterization of the active temperature control resulted in a working temperature of 26 °C with a resonance frequency of 9.998957 MHz and long-term stability of 0.1<°C/h. Meanwhile, some commercial devices like QSense Pro (Biolin Scientific) have similar long-term stability, with a long-term stability of <0.02C/h. Additionally, the system characterization data was contrasted with the openQCM Next (Open QCM) to confirm the efficiency showing a long-term stability <1 Hz/h and dissipation <0 0.15•10-6/h, just below what a commercial device offers.

Different PEG concentrations were analyzed as a validation procedure, showing an expected increase in resonance frequency and dissipation shift when the concentrations were higher. Results were more variable than expected regarding the marked difference between concentrations. Variations in measurements were shown to be due to the crystal cleaning process, due to impurities left on the crystal. The VNA software used in this article can show the real-time signal and does not include the option of obtaining the information from a continuous sweep. There are open source software such as Nano VNA Saver where modifications are allowed and could lead to saving the information in a continuous temporal sweep. Next steps will involve the study of the system performance in biomedical applications by using samples such as blood, human tears, bacteria and proteins.

Declaration of Competing Interest

The authors declare that they have no known competing financial interests or personal relationships that could have appeared to influence the work reported in this paper.

Acknowledgements

This work was supported by Agencia Nacional de Promoción Científica y Tecnológica, PICT StartUp 4655: Biosensor para la evaluación cualitativa y cuantitativa de la lágrima.

We want to thank to the Electronics Prototyping & 3D Lab of the National University of Entre Rios for giving us the facilities to develop and evaluate our prototype.

Appendix A

Supplementary data to this article can be found online at https://doi.org/10.5281/zenodo.7733393.

References

[1] P. Roriz, S. Silva, O. Frazao, Optical fiber temperature sensors and their biomedical applications, Sensors 20 (7) (2020) 2113, 10.3390%2Fs20072113.
[2] J. Xi, J.Y. Chen, M.P. García, L.S. Penn, Quartz crystal microbalance in cell biology studies, Biochips Tissue Chips (2013), https://doi.org/10.4172/2153-0777.S5-001.
[3] C. Fredriksson, S. Kihlman, M. Rodahl, B. Kasemo, The piezoelectric quartz crystal mass and dissipation sensor: a means of studying cell adhesion, Langmuir 14 (2) (1998) 248–251, https://doi.org/10.1021/la971005l.
[4] C. Tonda-Turo, I. Carmagnola, G. Ciardelli, Quartz crystal microbalance with dissipation monitoring: a powerful method to predict the in vivo behavior of bioengineered surfaces, Front. Bioeng. Biotechnol. 6 (2018), https://doi.org/10.3389/fbioe.2018.00158.
[5] N.A. Saad, S.K. Zaaba, A. Zakaria, L.M. Kamarudin, K. Wan, A.B. Shariman, Quartz crystal microbalance for bacteria application review. 2014 2nd International Conference on Electronic Design (ICED), (2014), 455-460. http://dx.doi.org/10.1109/ICED.2014.7015849.
[6] M.R. Eslami, N. Alizadeh, A dual usage smart sorbent/recognition element based on nanostructured conducting molecularly imprinted polypyrrole for simultaneous potential-induced nanoextraction/determination of ibuprofen in biomedical samples by quartz crystal microbalance sensor, Sens. Actuators B: Chem. 220 (2015) 880–887, https://doi.org/10.1016/j.snb.2015.06.017.
[7] Y.Y. Jia, Study on pivot-point vibration of molecular bond-rupture events by quartz crystal microbalance for biomedical diagnostics, Int. J. Nanomed. 7 (2012) 381–391, 10.2147%2FIJN.S26808.
[8] C.K. O'Sullivan, G.G. Guilbault, Commercial quartz crystal microbalances-theory and applications, Biosensors & Bioelectronics 14 (8-9) (1999) 663–670.

[9] A. Alassi, M. Benammar, D. Brett, Quartz crystal microbalance electronic interfacing systems: a review, Sensors (Switzerland) 17 (12) (2017), https://doi.org/10.3390/s17122799.
[10] S.N. Songkhla, T. Nakamoto, Signal processing of vector network analyzer measurement for quartz crystal microbalance with viscous damping, IEEE Sens. J. 19 (22) (2019) 10386–10392, https://doi.org/10.1109/JSEN.2019.2930733.
[11] K. Patel, P.S. Negi, P.C. Kothari, Complex S-parameter measurement and its uncertainty evaluation on a vector network analyzer, Measurement 42 (1) (2009) 145–149, https://doi.org/10.1016/j.measurement.2008.04.010.
[12] F. Neumann, N. Madaboosi, I. Hernández-Neuta, J. Salas, A. Ahlford, V. Mecea, M. Nilsson, QCM mass underestimation in molecular biotechnology: proximity ligation assay for norovirus detection as a case study, Sens. Actuators B: Chem. 273 (2018) 742–750, https://doi.org/10.1016/j.snb.2018.06.025.
[13] A.J. Olsson, I.R. Quevedo, D. He, M. Basnet, N. Tufenkji, Using the quartz crystal microbalance with dissipation monitoring to evaluate the size of nanoparticles deposited on surfaces, ACS Nano 7 (9) (2013) 7833–7843, https://doi.org/10.1021/nn402758w.
[14] M.J. Swann, The Principles of QCM-I. https://mmrc.caltech.edu/Gamry/manuals/QCM-I-principles.pdf.
[15] F. Caspers, RF engineering basic concepts: S-parameters.(2012). https://doi.org/10.48550/arXiv.1201.2346.
[16] S. Na Songkhla, T. Nakamoto, Interpretation of quartz crystal microbalance behavior with viscous film using a mason equivalent circuit, Chemosensors 9 (9) (2021), https://doi.org/10.3390/chemosensors9010009.
[17] M. Rodahl, F. Höök, C. Fredriksson, C.A. Keller, A. Krozer, P. Brzezinski, M. Voinova, B. Kasemo, Simultaneous frequency and dissipation factor QCM measurements of biomolecular adsorption and cell adhesion, Faraday Discussions 107 (1997) 229–246, https://doi.org/10.1039/a703137h.
[18] A. Itoh, M. Ichihashi, Separate measurement of the density and viscosity of a liquid using a quartz crystal microbalance based on admittance analysis (QCM-A), Measure. Sci. Technol. 22 (1) (2011) 015402, https://doi.org/10.1088/0957-0233/22/1/015402.
[19] A. Cao-Paz, L. Rodriguez-Pardo, J. Fariña, Temperature compensation of QCM sensors in liquid media, Sens. Actuators, B: Chem. 193 (2014) 78–81, https://doi.org/10.1016/j.snb.2013.11.044.
[20] Y. Tsuchiya, H. Kukita, T. Shiobara, K. Yukumatsu, E. Miyazaki, Temperature Controllable QCM Sensor with Accurate Temperature Measurement for Outgas and Contamination Assessment. 2019 IEEE Sensors, (2019), 1-4. https://doi.org/10.1109/SENSORS43011.2019.8956952.
[21] C. Koçum, A. Erdamar, H. Ayhan, Design of temperature controlled quartz crystal microbalance system, Instrument. Sci. Technol. 38 (1) (2010) 39–51, https://doi.org/10.1080/10739140903427137.
[22] M.A. Amer, J.A. Chávez, M.J. García-Hernández, J. Salazar, A. Turó, Quartz crystal microbalance holder design for on-line sensing in liquid applications, Int. J. Electric. Comput. Eng. 10 (5) (2016) 684–687, https://doi.org/10.5281/zenodo.1124449.
[23] D. Meléndrez, P. Hampitak, T. Jowitt, M. Iliut, A. Vijayaraghavan, Development of an open-source thermally stabilized quartz crystal microbalance instrument for biomolecule-substrate binding assays on gold and graphene, Analytica Chimica Acta 1156 (2021) 338329.
[24] T.-R. Yan, C.-F. Lee, H.-C. Chou, QCM as Cell-Based Biosensor, in: D. Ekinci (Ed.), Chemical Biology, InTech, 2012, https://doi.org/10.5772/34261.
[25] P. Hampitak, T.A. Jowitt, D. Melendrez, M. Fresquet, P. Hamilton, M. Iliut, K. Nie, B. Spencer, R. Lennon, A. Vijayaraghavan, A point-of-care immunosensor based on a quartz crystal microbalance with graphene biointerface for antibody assay, ACS Sens. 5 (11) (2020) 3520–3532, https://doi.org/10.1021/acssensors.0c01641.
[26] W. Shinobu, H. Kukita, S. Wakamatsu, Review about the development of the differential expression QCM system, Electron. Commun. Japan 101 (3) (2018) 66–72, https://doi.org/10.1002/ecj.12038.
[27] S. Turkdogan, Design and implementation of a cost effective quartz crystal microbalance system for monitoring small changes on any surface, Balkan J. Electric. Comput. Eng. (2019) 213–217, https://doi.org/10.17694/bajece.530796.

G.G. Muñoz I am a young doctoral student working at the Laboratory of Electronic Prototyping and 3D (LEP3D), Faculty of Engineering, National University of Entre Ríos (UNER), Argentina. I am 32-years-old-Bioengineer fascinated by the discovery of new knowledgement and its application in the real world. I am currently working on innovations in the field of dry eye by using a quartz crystal microbalance.

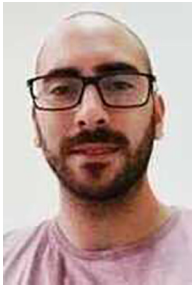

M.J. Millicovsky I am a young scientist studying the behavior of acoustic wave resonators for biomedical applications at. I work as a PhD scholar at the Institute for Research and Development in Bioengineering - National Council for Scientific and Technical Research (IBB-CONICET). I am 28 years old Electronic Engineer from the National Technological University - Paraná Regional Faculty (UTN-FRP) and my passion is to investigate new and challenging topics, as well as participate in the development of useful devices to carry out different experiments. I am currently studying Love surface acoustic wave resonators (LSAW) for the analysis of human tears, thus helping the diagnosis of dry eye syndrome.

M.A. Zalazar I am a Bioengineer from National University of Entre Rios (UNER) and have a PhD in Engineering Sciences from National University of Litoral (UNL). My research interests are related with the design, simulation, fabrication and characterization of BioMEMS/NEMS focused on microsensors for mass, and biomolecules detection using piezoelectric materials (AlN, PVDF and quartz), as well as microfluidic and electronic & 3D print prototyping for biomedical applications. Being a Technology Researcher, I've created a healthtech Startup.